

# Estimation of scattering and chromophore concentration maps by multi-band spatial frequency domain imaging using a two-layer skin model

Yuto Shimada<sup>1</sup>, Yu Feng<sup>1</sup>, Chen Cao<sup>2</sup>, Keita Yasutomi<sup>2</sup>, Shoji Kawahito<sup>2</sup>, Keiichiro Kagawa<sup>2</sup>

<sup>1</sup> Graduate School of Integrated Science and Technology, Shizuoka University

3-5-1 Johoku, Hamamatsu, 432-8011 Japan

<sup>2</sup> Research Institute of Electronics, Shizuoka University

3-5-1 Johoku, Hamamatsu, 432-8011 Japan

E-mail: kagawa@idl.rie.shizuoka.ac.jp

**Abstract** Spatial frequency domain imaging (SFDI) can perform simultaneous quantitative measurement of the distributions of reduced scattering coefficient and chromophore concentrations of tissues by using multi-band images. We have previously proposed a multi-band SFDI system using a multi-tap CMOS image sensor to suppress the ambient light and motion artifacts. In order to perform quantitative skin measurements using this system, we have developed a method for estimating the distributions of melanin, total hemoglobin, tissue oxygen saturation, and scattering parameters of the human forearm using the illumination wavelengths of 660, 780, and 850 nm, based on a two-layer skin model.

**Keywords:** spatial frequency domain imaging, Monte Carlo Simulation, multi-tap CMOS image sensor, diffuse optics, skin

## 1. Introduction

Spatial frequency domain imaging (SFDI) is a non-invasive, non-contact, video-rate quantitative wide-field imaging method for the absorption coefficient  $\mu_a(\lambda)$  and the reduced scattering coefficient  $\mu'_s(\lambda)$  of tissues [1]. SFDI can perform simultaneous quantitative measurements of the distributions of reduced scattering coefficient and chromophore concentrations of tissues by using multi-band images. Therefore, it is promising for various applications such as burn severity diagnosis [2], imaging of brain activity [3], and so on. However, SFDI is affected by ambient light and motion artifacts. In addition, because the measured information is basically diffuse reflectance, the estimated optical parameters and chromophore concentrations are dependent on tissue modeling. Actual tissues are multi-layered and different for the parts of the body. Therefore, multi-layered modeling of the tissue to suit the target is unavoidable.

We have previously proposed a multi-band SFDI system using a multi-tap CMOS image sensor to suppress the ambient light and motion artifacts [4]. One of the problems with this system is the low estimation accuracy caused by a bulk model.

In order to perform accurate quantitative skin measurements using this system, we have adopted a two-layer skin model for estimating the distributions of melanin, total hemoglobin, tissue oxygen saturation, and scattering parameters of the human forearm using the illumination wavelengths of 660, 780, and 850 nm.

## 2. Multi-band SFDI with a two-layered skin model

SFDI is based on the fact that the modulation transfer function (MTF) of a diffusive medium depends on  $\mu_a(\lambda)$  and  $\mu'_s(\lambda)$ . Typically, the MTF for two or more spatial frequencies is measured at every pixel. Then,  $\mu_a(\lambda)$  and  $\mu'_s(\lambda)$  are estimated by referring to a look-up table (LUT) made by the Monte Carlo simulation. For measuring the MTF, three sinusoidal patterns with a one-dimensional wave vector whose spatial phases differ by  $2\pi/3$  are projected to the tissue, and their reflection images are taken. When the pixel values of the reflection images for the three spatial phases are denoted by  $I_1(x, y)$ ,  $I_2(x, y)$ , and  $I_3(x, y)$ , the amplitudes of reflection for AC and DC components,  $M_{ac}$  and  $M_{dc}$ , are calculated by Eqs. 1 and 2, respectively.

$$M_{ac} = \frac{\sqrt{2}}{3} [\{I_1(x, y) - I_2(x, y)\}^2 + \{I_2(x, y) - I_3(x, y)\}^2 + \{I_3(x, y) - I_1(x, y)\}^2]^{\frac{1}{2}} \quad (1)$$

$$M_{dc} = \frac{1}{3} [I_1(x, y) + I_2(x, y) + I_3(x, y)] \quad (2)$$

Multi-band imaging enables us to estimate chromophore concentrations such as oxy-/deoxy-hemoglobin, melanin, fat, and water by fitting the measured absorption spectrum with a linear combination of their known molar extinction coefficient of absorbers [5].

The two-layer skin model was assumed to mimic the epidermis and dermis. In this model, we assumed that melanin is distributed in the epidermis and hemoglobin in the dermis [6]. The absorption coefficient of each layer is defined by Eqs. 3 and 4, respectively. The subscripts m, hbo and hbd for molar extinction coefficient  $\epsilon(\lambda)$  denote the melanin [7], oxygenated hemoglobin, and deoxygenated hemoglobin [8], respectively.  $C_m$ ,  $C_{hbt}$ , and  $StO_2$  denote melanin concentration [%], total hemoglobin [ $\mu M$ ], and tissue oxygen saturation [%], respectively. The reduced scattering coefficients of the two layers are assumed to be the same. The reduced scattering coefficient of skin is assumed to follow the power law for wavelength and can be fitted by Eq. 5 [9]. To estimate the concentrations of melanin, hemoglobin, and the reduced scattering, we calculated the MTF by Monte Carlo simulation [10] and made a LUT for the combinations of scattering parameters  $a$  [ $mm^{-1}$ ],  $b$ , total hemoglobin  $C_{hbt}$ , tissue oxygen saturation  $StO_2$ , and melanin concentration  $C_m$  shown in Table 1.

$$\mu_{a,epi}(\lambda) = \epsilon_m(\lambda) \times C_m \quad (3)$$

$$\mu_{a,der}(\lambda) = \ln(10) \times C_{hbt} \times \{StO_2 \times \epsilon_{hbo}(\lambda) + (1 - StO_2) \times \epsilon_{hbd}(\lambda)\} \quad (4)$$

$$\mu'_{s,epi}(\lambda) = \mu'_{s,der}(\lambda) = a \times \left(\frac{\lambda}{500 \text{ nm}}\right)^{-b} \quad (5)$$

Table 1 Parameter ranges for Monte Carlo simulation

$a$ [ $\text{mm}^{-1}$ ]	2.1		4.2			8.4		
$b$	1		2			3		
$C_{\text{hbt}}$ [ $\mu\text{M}$ ]	4.6	23	69	115	161	207	253	300
StO <sub>2</sub> [%]	20		50			80		
$C_m$ [%]	0	2	5	8				

### 3. Experimental results

In the experiments, we used 660, 780 and 850 nm LEDs as the light sources of the DMD projector to project a sinusoidal pattern onto the specimen. We measured a human forearm using a commercial CMOS image sensor (XIMEA, MQ013RG-E2).

Fig. 1 shows the calculated results of Mdc and Mac at each wavelength. The reflectance images are slightly different at different wavelengths. Mdc and Mac depict deep and shallow blood vessels, respectively.

Fig. 2 shows the estimated maps with a two-layer skin model. In the maps of melanin, estimated values are higher in the body hair area. Note that its distribution is also different from the vascular pattern. This indicates that melanin is separated from hemoglobin successfully.

The total hemoglobin map shows both the deep vascular pattern taken with the Mdc and the shallow vascular pattern by Mac. The map of tissue oxygen saturation and scattering parameter  $a$  shows a relatively uniform distribution. The scattering parameter  $b$  corresponds to the particle size of diffusive media.  $b$  is close to 1 in the hairy and wrinkled areas and about 2 in the shallow blood vessels.

### 4. Conclusion

We have developed a method for estimating the distributions of melanin, total hemoglobin, tissue oxygen saturation, and scattering parameters on the human forearm based on a two-layer skin model. Experimental results showed good separation of melanin and hemoglobin. The estimated parameters were reasonable compared with those in the literature.

### Acknowledgement

This work was supported in part by JSPS KAKENHI Grant Number JP21H04557.

### References

[1] S. Gioux, A. Mazhar and D. J. Cuccia: "Spatial frequency domain imaging in 2019: principles, applications and perspectives", *J. Biomed. Optics*, 24, 7, 071613 (Jul. 2019).

[2] A. Ponticorvo, R. Rowland, M. Baldado, G. T. Kennedy, Anna-Marie Hosking, D. M. Burmeister, R. J. Christy, N. P. Bernal, A. J. Durkin: "Spatial Frequency Domain Imaging (SFDI) of clinical burns: A case report", *Burns Open* Vol. 4, Issue 2, Pages 67-71 (April 2020).

[3] R. P. Singh-Moon D. M. Roblyer, I. J. Bigio, S. Joshi, "Spatial mapping of drug delivery to brain tissue using hyperspectral spatial frequency-domain imaging", *J. Biomed. Opt.* 19(9), 096003 (2014).

[4] K. Takada, Y. Shimada, K. Yasutomi, S. Kawahito, G. T. Kennedy, A. J. Durki, K. Kagawa: "Demonstration of 3-band spatial frequency domain imaging using an 8-tap CMOS image sensor resistant to subject motion and ambient light", *Proc. SPIE* 11951, Design and Quality for Biomedical Technologies XV, 1195106 (2 March 2022).

[5] A. Mazhar, S. Dell, D. J. Cuccia, S. Gioux, A. J. Durkin, J. V. Frangioni, and B. J. Tromberg: "Wavelength optimization for rapid chromophore mapping using spatial frequency domain imaging", *Journal of Biomedical Optics*, Vol. 24, No. 4, pp. 639-

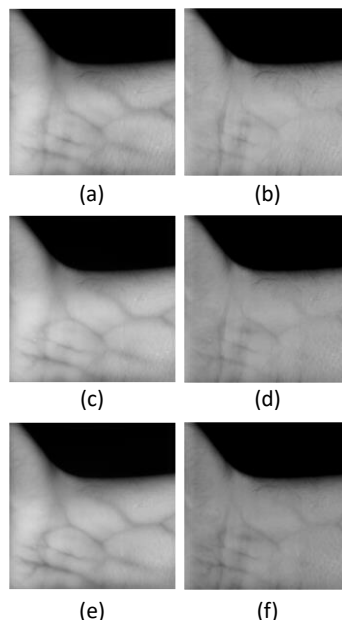


Fig. 1. Calculated results of (a)(c)(e) Mdc and (b)(d)(f) Mac. (a)(b) 660nm. (c)(d) 780nm. (e)(f) 850nm.

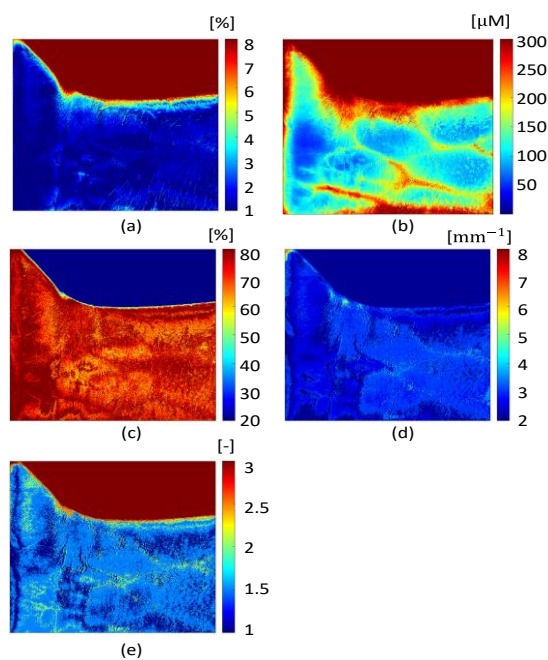


Fig. 2. Estimated maps of (a) melanin, (b) total-hemoglobin, (c) tissue oxygen saturation, (d) scattering parameter  $a$ , and (e) scattering parameter  $b$

651 (2009).

[6] S. L. Jacques: "Melanosome Absorption Coefficient", <https://omlc.org/spectra/melanin/mua.html>

[7] S. Prahl: "Tabulated Molar Extinction Coefficient for Hemoglobin in Water", <https://omlc.org/spectra/hemoglobin/summary.html>

[8] S. L. Jacques: "Skin optics", Oregon Medical Laser Center News, <https://omlc.org/news/jan98/skinoptics.html>

[9] S. L. Jacques: "Optical properties of biological tissues: a review", *Phys. Med. Biol.* 58, R37–R61 (2013).

[10] Q. Fang and D. Boas: "Monte Carlo Simulation of Photon Migration in 3D Turbid Media Accelerated by Graphics Processing Units", *Opt. Express*, vol. 17, issue 22, pp. 20178-20190 (2009).